Chemical Science

Accepted Manuscript

This article can be cited before page numbers have been issued, to do this please use: W. Wong, D. Phillips, M. T. Rahman and T. Junkers, *Chem. Sci.*, 2026, DOI: 10.1039/D5SC07307C.

ROYAL SOCIETY OF CHEMISTRY

rsc.li/chemical-science

View Article Online
DOI: 10.1039/D5SC07307C

ARTICLE

Automated Closed-Loop Continuous Flow Block Copolymer Synthesizer

Received 00th January 20xx,
Accepted 00th January 20xx

DOI: 10.1039/x0xx00000x

Wei Nian Wong,[a] Daniel J. Phillips,[b] Md Taifur Rahman[b] and Tanja Junkers [*,a]

A fully automated continuous flow synthesizer for diblock copolymer (BCP) synthesis was constructed comprising elements of flow chemistry, automation, machine learning and in-line monitoring. A new method using in-line FTIR spectroscopic analysis for accurate determination of monomer conversion (with error as low as 2 % relative to an NMR spectroscopic baseline) is presented which generates a reliable feedback system for reaction self-optimisation using the platform. By employing reversible addition-fragmentation chain transfer (RAFT) polymerization at 100 °C, acrylates and acrylamides of different hydrophilicities (namely methyl acrylate, ethyl acrylate, butyl acrylate, 2-ethylhexyl acrylate, 2-hydroxyethyl acrylate, ethylene glycol methyl ether acrylate, diethylene glycol ethyl ether acrylate, 2-(dimethylamino)ethyl acrylate, acrylamide & N,N-dimethylacrylamide) were polymerized to make mixed BCPs, targeting different degrees of polymerization (15 to 100). Samples were collected automatically and a BCP material library comprising 95 diblock copolymers (7 sets of double hydrophobic, 7 sets of amphiphilic and 3 sets of double hydrophilic monomer systems) with M_n ranging from 1 800 g·mol^{-1} to 14 700 g·mol^{-1}, was obtained in a high throughput manner, with minimal human intervention throughout the entire process.

Introduction

Block copolymers (BCPs) exhibit a broad variety of compositions and microstructures, making them an exciting class of adaptable material with many applications across the biomedical field,[1] stimuli-response nanoparticles for drug delivery application,[2] nanofabrication for electronic applications,[3] and membrane technology for environmental applications.[4] Microphase separation in polymer self-assembly due to chemical dissimilarity of the individual blocks is also a unique characteristic that differentiates them from simpler polymers.[5] The discovery of reversible deactivation radical polymerization (RDRP) has accelerated the synthesis of well-defined BCPs, and opened the door for the synthesis of polymers with increasingly complex architectures. Among the different RDRP techniques, reversible addition-fragmentation chain transfer (RAFT) polymerization holds a fortified position for block copolymer synthesis due to its high efficiency when operated under correct conditions, and its applicability to a broad range of monomers, solvents and process conditions.[6]

Despite the attractive properties of block copolymers, most industrial polymer applications are still dominated by conventional homopolymers and statistical copolymers, which is at least in part due to the significant hurdles associated with exploring new classes of materials. Even if RAFT polymerization is simple, it presents an increased cost and research and development burden. To challenge this status quo, there is a crucial need to streamline the material discovery process, and this is where flow chemistry and reaction automation can play a significant role. In comparison to batch chemistry, flow chemistry offers superior heat and mass transfer within a given reaction space, ease of reactor scale-up, high reproducibility of experimental results and inherently safer operability.[7, 8] These advantages make flow reactors an ideal platform with which to develop novel materials on scale in a cheaper and more time-efficient manner. Furthermore, the integration of real-time monitoring tools allows for rapid acceleration of research activity and enables high-throughput experimentation and analysis, providing the basis for powerful reaction automation. Examples of online monitoring techniques which find application in the polymer chemistry domain include nuclear magnetic resonance (NMR) spectroscopy,[9-12] infrared (IR) spectroscopy,[13] size exclusion chromatography (SEC)[14] and electrospray ionization mass spectrometry (ESI-MS).[15]

Although the synthesis of block copolymers *via* a flow setup has been demonstrated before,[16-21] a considerable amount of manual work is still required throughout the process, from varying the flow rate of a reaction stream to reaction sampling. For instance, Vandenbergh *et al.* synthesized various RAFT pentablock copolymers in a microchip reactor. However, each

[a] *Polymer Reaction Design Group, School of Chemistry, Monash University, 19 Rainforest Walk, Building 23, Clayton, VIC 3800, Australia. E-mail: tanja.junkers@monash.edu.*
[b] *Infineum International Ltd., Milton Hill Business and Technology Centre, Abingdon. OX13 6BD, United Kingdom.*

† Footnotes relating to the title and/or authors should appear here.
Supplementary Information available: [details of any supplementary information available should be included here]. See DOI: 10.1039/x0xx00000x

View Article Online
DOI: 10.1039/D5SC07307C

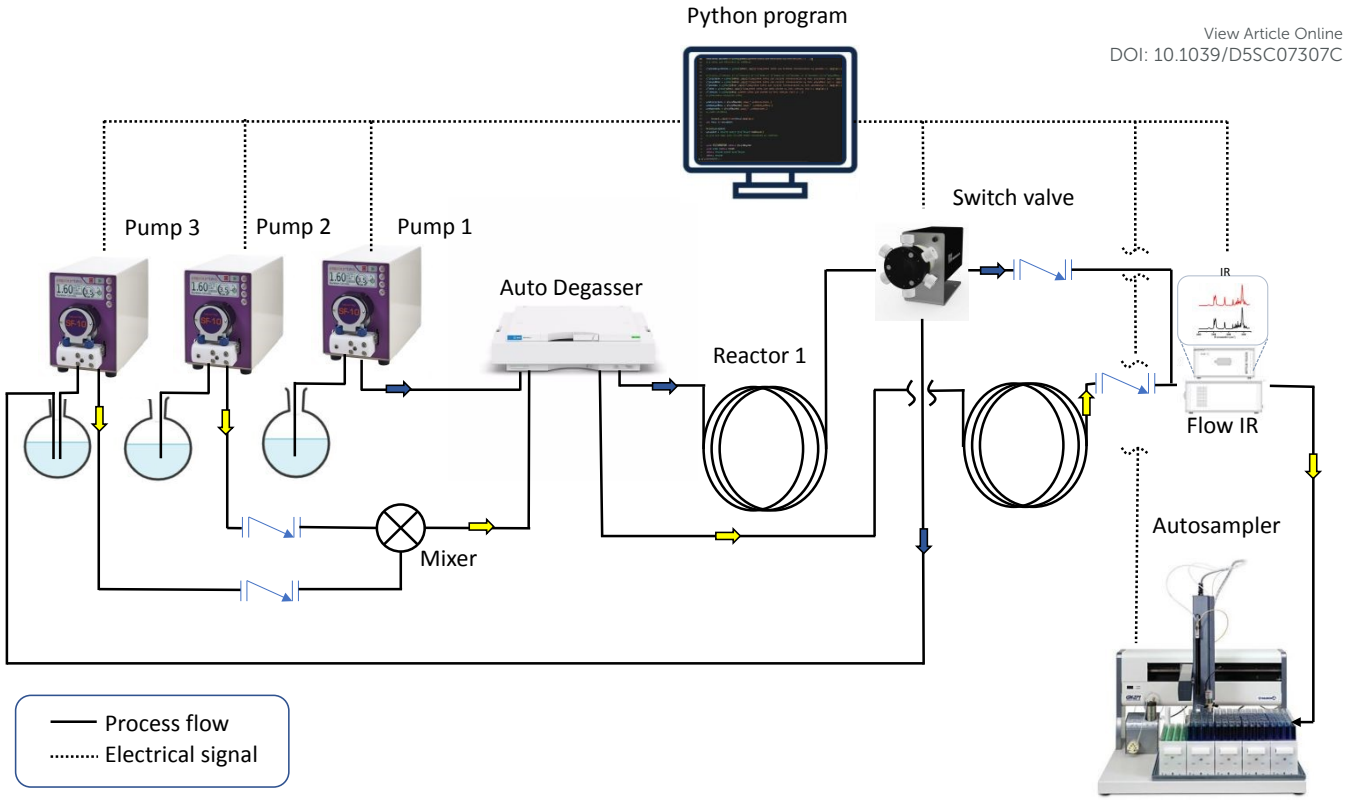

Fig 1: Schematic diagram of the presented fully automated diblock copolymer synthesizer. Blue and yellow arrows indicate the process flow for the synthesis of homopolymer and diblock copolymer, respectively. The setup is constructed for two tubular reactors that are fully submerged in oil baths, three peristaltic pumps, an auto degasser, an FTIR spectroscopic monitor with flow cell and a liquid handling autosampler. Dotted lines indicate instruments that are communicating with the Python program and are actively involved in the automation while solid lines indicate the process streams.

block required isolation and purification before subsequent chain-extension, introducing discontinuity in the process flow, potential error from human intervention and a notable increase in operation time.[20] Hornung *et al.* utilized a commercially available flow system to produce block copolymers without the need for isolation. However, the flexibility of this approach is limited by the inability to change the volume of reactors and hence residence times in the second reactor.[16] On the other hand, Perrier and co-workers constructed a looped flow reactor. By dosing monomers into the loop at different phases of the experiment, multiblock copolymers were successfully synthesized using just one tubular reactor.[22] The same objective was achieved by Baeten *et al*. *via* a continuous multistage reactor cascade for high throughput synthesis of multiblock copolymers. Although sophisticated, the aforementioned approaches could only produce one specific block copolymer per experiment, limiting its use as a high throughput synthesis tool.[18] Moreover, none of these reports integrate real-time monitoring into their system. Therefore, the volume of polymerization kinetic data collected was limited and no automated data processing could occur, hence relying on constant human intervention to adapt reaction conditions. Generally, the integration of real-time monitoring tools into flow synthesis establishes an instant feedback system which enables autonomous closed loop experimentation. In such systems, reaction parameter(s) can be improved iteratively by utilization of machine learning or other user-defined decision-making algorithms to satisfy a pre-defined objective function.[10, 23, 24] The power of inline and online tools for the monitoring of polymerization kinetics has also been demonstrated. For instance, Van Herck *et al.* created a fully automated setup for real-time polymerization monitoring with in-line NMR spectroscopy and online SEC. The robustness of the approach was demonstrated by multiple users creating coherent datasets without prior training.[9, 25] Within the same group, Zhang *et al.* also demonstrated the application of inline IR spectroscopy for the rapid screening of RAFT reaction parameters in a high throughput manner.[13] Rubens *et al.* were among the first to use online monitoring to achieve closed-loop experimentation in the domain of polymer chemistry, where a self-optimizing reactor was created to target different monomer conversions.[10] By using similar analytical instruments, the same objective was also achieved by the Warren group, additionally introducing multiparameter Bayesian optimization to guide the reaction screening and optimization process.[23, 26]

While these closed loop reactors are highly interesting for the production of individual polymers under specific conditions, approaches to the rapid production of wider functional sample libraries would further accelerate the development of new materials. To achieve this, a combination of self-optimization algorithms with robotic high-throughput experimentation is required. Herein, we describe such a combination, presenting a high-throughput, fully automated block copolymer

synthesizer. To demonstrate its versatility, we utilized the system to construct a library of diblock copolymers combining a range of acrylate and acrylamide monomers to make polymers of a variety of chain lengths. With the concept of the "frugal twin" in mind,[27] we constructed the setup with easily accessible lab tools that will allow similar machines to be installed elsewhere at reasonable cost. A schematic of the BCP synthesizer is outlined in **Fig. 1**. The machine comprises two reactor loops for homopolymer synthesis and successive chain extension, three peristaltic pumps to deliver reagents and solvent, and a robotic sample collector to store the obtained BCPs. To ensure continuous end-to-end operation for the machine and allow for self-optimization, a master Python program was written to control the hardware elements and also to collect, process and model kinetic data throughout the entire experiment. With the integration of in-line infrared spectroscopy, instant access to kinetic information is available throughout the experiment, which will be exploited by a decision-making algorithm to improve the process conditions autonomously. Finally, the synthesizer has not only the capacity to generate a diverse library of diblock copolymers, consisting of double hydrophilic, double hydrophobic and amphiphilic nature, it also provides high density kinetic data for each of the reactions, enabling future data driven applications.

Experimental

Reactor set-up

Two tubular reactors (3 ml for first block and 3.4 ml for second block), constructed from fluorinated gastight PFA tubing (1/16'' OD, 0.75 mm ID), were formed into loops and fully submerged in two mineral oil baths, which were heated to 100 °C on an IKA RCT hot plate. The volume of both reactors was designed to be larger than those that were previously employed in our group,[10,18] with the intention to reduce both the macro-RAFT agent collection time (first reactor) and the sampling time for each diblock copolymer (second reactor). Other passive volumes (where no reaction happens) that connected all the process units in the setup were introduced using tubing of the same material and dimensions, including a sampling loop (1.4 ml) for BCP collection before dispensing into vials by the autosampler. Three Vapourtec SF10 peristaltic pumps were used to control the flow rates of stock solution 1 (Pump 1), stock solution 2 (Pump 2) and macro-RAFT agent (Pump 3) respectively. A switch valve (Valco C4UWE Valve) was connected to the outlet of reactor 1 to direct its stream towards either (a) the IR flow cell or (b) a macro-RAFT reservoir. A Y-piece mixer (Y Assembly PEEK cd1/4-28 .020 in) was used to merge macro-RAFT agent and stock solution 2 streams before passing into a degasser (Agilent 1260 Infinity). A liquid-handling autosampler (Gilson, GX-271) was connected to the outlet of the IR flow cell (Mettler Toledo ReactIR) for sampling of the polymers. Two check valves were placed downstream of both reactors to prevent backflow when either of them was directed towards the IR flow cell for kinetic monitoring. A Stock solution 1 was prepared by mixing the monomer of choice, 2-(dodecylthiocarbonothioylthio) propionic acid (DoPAT) and 1,1'-azobis(isobutyronitrile) (AIBN) in butyl acetate while stock solution 2 contained a different monomer and no RAFT agent (all details on parts used and further experimental details are found in the SI).

Reactor process flow

The automated setup is fully controlled by a master Python script and when initiated, the user is asked to input several parameters including stock solution concentrations, desired target degree of polymerization (DP_{Target}) for the first and second blocks, types of monomers involved, residence times for timesweep screening, and the target conversion for the first block. Other parameters like reactor or other non-reaction dimension (sampling volume, dead volume), IR scan interval etc. can also be changed (without prompt) when alterations to the setup are made (which, for example, may occur for maintenance reasons).

The process starts with the degassing of stock solution 1. This occurs *via* passing the reaction mixture into the auto-degasser unit for oxygen removal. After all the non-reaction volume is filled with deoxygenated reaction mixture, the program will then proceed to initiate a transient timesweep kinetic screening experiment according to the residence times inputted by the user. The timesweep screening experiment, made possible by the integration of an in-line monitoring tool, collects kinetic data during transient periods in the reaction (i.e. when the flow rate changes within the tubular reactor) in-line. Assuming the process operates in a plug flow regime, each plug is subjected to a different residence time, thus providing a comprehensive kinetic profile as the reactor ramps between the inputted start and end residence times.[9, 28] At the end of the timesweep experiment all raw IR data is processed and the kinetic model exported in a comma separated values (csv) file. After this initial fast screen, the setup then switches automatically into a self-optimizing loop. Based on the timesweep data, a polymerization will be carried on the basis of the prediction made from the kinetic model. The monomer conversion value will then be compared the target conversion, and the model updated if required. This cycle will repeat to fine tune the kinetic model iteratively until the target is achieved. Upon successful achievement of the target conversion, the switch valve will direct the outlet of reactor 1 towards a macro-RAFT reservoir (connected to pump 3), and the setup will switch into macro-RAFT synthesis mode, at the optimal residence time. Afterwards, the setup will synthesize 15ml of macro-RAFT before proceeding to the next step, to ensure a sufficient quantity is available for the next screening process.

The process flow for the second block is roughly the same as the first part of the Python script, except two pumps (pump 2 and 3) are required to control the flow rates of both macro-RAFT agent and stock solution 2. An autosampler downstream of the IR detector will collect samples during the stabilization period of the timesweep experiment, which are later analysed via NMR and SEC for their monomer conversion and relative molar mass distributions (MMD). Details of the NMR and SEC analysis used for this study are available in the **Supporting Information (SI)**. The SEC system was calibrated using PMMA standards, and

View Article Online DOI: 10.1039/D5SC07307C

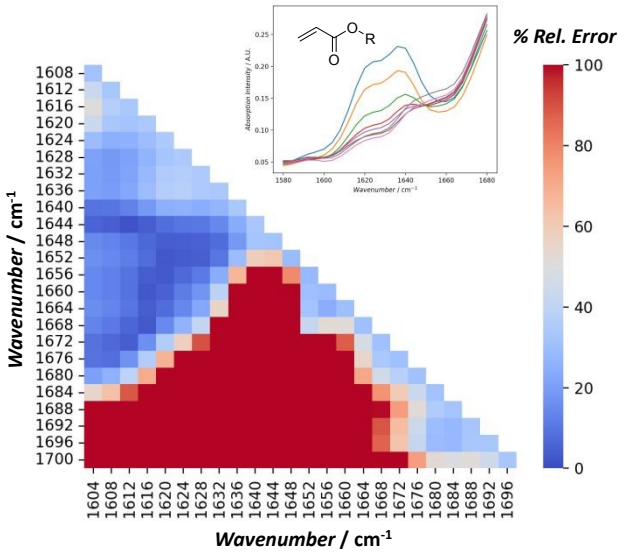

Monomer	Solvent	Wavenumber Range/cm^{-1}	Relative Error/ %
Ethyl acrylate	Butyl acetate	1652-1620	1.94
	n-Butanol	1668-1648	3.48
Methyl acrylate	Cyrene	1648-1624	4.43
Butyl acrylate	Butyl acetate	1656-1624	7.63
2-Ethylhexyl acrylate		1660-1608	11.85
Diethylene glycol ethyl ether acrylate		1660-1612	1.72
Ethylene glycol methyl ether acrylate		1660-1616	7.38
Poly(ethylene glycol) methyl ether acrylate		1664-1648	7.83

Fig 2: Heatmap of the relative error (in %), calculated based on the peak area integrated over different ranges of wavenumber on the IR spectra, from 1700 cm^{-1} to 1600 cm^{-1}, and compared with the conversion values from NMR analysis, for all the collected. Table: Optimal wavenumber range for quantitative analysis of residual monomers, covering a range of acrylic monomers in various solvents.

molar masses given are relative to these standards. These characterization results are complemented by the comprehensive kinetic data collected using IR spectroscopy throughout the experiment.

Results and discussion

Tracking monomer conversion by FTIR spectroscopy: Determining an optimal wavenumber (WN) range for quantitative analysis

In order to use IR spectroscopy as an inline monitoring tool for reaction kinetic monitoring, we need to establish a calibration model for monomer consumption. This can be achieved by monitoring the change in IR frequencies associated with the monomer vinyl group. Peaks at 1630 cm^{-1} and 819 cm^{-1}, which correspond to C=C bond stretching and twisting motions respectively, are suitable for this purpose; the former frequency is particularly preferable owing to its stronger absorption intensity and lower sensitivity to any fluctuation in ambient conditions.[29-31] Multiple point calibration models for a chemical system usually require frequent maintenance as they are prone to systematic errors due to fluctuations in chemical and physical characteristics of the chemical system and the analytical instrument. The deviation from Beer-Lambert's law necessitates the introduction of a correction coefficient to the evaluation. Additionally, the baseline drawn (between two wavenumbers) on the selected IR peak for integration has significant impact on the obtained result and is always a subjective choice for different researchers.[32]

Using monomer conversion determined via NMR spectroscopy as a comparative benchmark, we applied a data science approach to determine a suitable IR wavenumber (WN) range,

Table 1: Homopolymerization and diblock copolymerization of various acrylates and acrylamides via DoPAT-mediated RAFT polymerization. Different DP_{Target} were targeted by adjusting the $[M]_0/[CTA]$, while the starting monomer concentration was varied according to the bulkiness of the monomer involved and its corresponding initiator concentration was set to maintain a consistent reaction rate.

	Monomer	$[M]_0$ / M	$[M]_0$ / $[I]_0$	DP_{target}
First Block	Ethyl acrylate (EA)	4	500	15-75
	Diethylene glycol ethyl ether acrylate (DEGEEA)	3		50
	Ethylene glycol methyl ether acrylate (EGMEA)	4		30
Second Block	Methyl acrylate (MA), butyl acrylate (BA), 2-ethylhexyl acrylate (EHA), 2-hydroxyethyl acrylate (HEA), DEGEEA, acrylamide (AC), N,N-dimethylacrylamide (DMAC)	2	750	30-75
	$PEGMEA_{480}$	1		30
	2-(Dimethylamino)ethyl acrylate (DMAEA)	2	300	30

View Article Online
DOI: 10.1039/D5SC07370

while maintaining good linearity with the Beer-Lambert law. To this end, the systematic screening of WN ranges between 1700 cm^{-1} and 1600 cm^{-1} was carried out. The approach performs max-min normalization with the IR spectra of the initial stock solution sample to account for the fluctuation in ambient conditions that may affect the IR background. The optimal WN range for different acrylates and solvents was calculated based on polymerization samples collected in a prior experiment and a Python algorithm was developed for the screening process to generate a heatmap, showcasing the discrepancy in values across different WN ranges. The WN range which showed the lowest error relative to the NMR spectroscopic baseline was chosen and implemented in the master Python program for automatic conversion determination.

The left-hand side of **Fig 2** shows an example of such a heatmap, based on experimental samples collected from the RAFT polymerization of ethyl acrylate (monomer) in butyl acetate (solvent). The dark blue region highlights the WN range (1660 cm^{-1} – 1612 cm^{-1}) that showed lowest error in measured conversion relative to NMR spectroscopic analysis, while the dark red region shows the highest error (> 70 %). 1652 cm^{-1} - 1620 cm^{-1} was therefore selected for analysis as it shows the lowest error (1.92 %), which is within the accuracy of a typical NMR spectroscopic experiment, and also comparable to the error range (< 5 %) demonstrated by previous work done within our group.[13] A comparative study was also carried out using a predetermined IR calibration curve to quantify the monomer conversion for three different experiments (operated under different temperatures of 90 to 110 °C). Experimental samples were collected and analysed by NMR spectroscopy, and the average discrepancy was 6.68 % (**Table S4)**. The optimal WN range and the respective relative error for each of the acrylate monomers applied in this study under various solvents is shown on the right-hand side of **Fig 2**. The error obtained via the FT-IR analysis is larger for acrylates like 2-EHA (11.85 %), PEGMEA (7.83 %), EGMEA (7.38 %) and BA (7.63 %), which could be due to errors in the NMR spectroscopic method used or due to insufficient calibration points in the FT-IR spectra**.** This could be, partly attributed to lower starting monomer concentration when bulkier monomers are used (1M for PEGMEA and 3M for EHA), and continue to decrease throughout polymerization. Consequently, a higher margin of error for FTIR analysis at such low concentrations is not uncommon.[13] The details for homopolymerization conditions is provided in Supporting Information (Table S4). Among the other contributing factors are interaction between monomers and solvents that can lead to shifts in spectral peaks[33] and variations in the viscosity of reaction mixtures, which has a pronounced effect on the hydrodynamic flow profile within the reactor and sampling tube. On the other hand, it should be noted that only 4-5 samples were typically collected for NMR spectroscopic analysis so the associated error could be reduced further by increasing the number of samples taken.

Reaction design

In a typical multiblock reactor telescoping reaction, it is a requirement that each of the polymerization steps achieves full monomer conversion prior to chain extension in the subsequent unit. This is to avoid quasi-block copolymer formation due to incorporation of the residual monomer from the upstream unit into the second block.[34, 35] To maximize monomer conversion, the temperature was set to 100 ˚C. Despite the positive impact of high operating temperature on the polymerization rate, consideration has to be taken with respect to side reactions such as mid-chain radical formation[7] and the initiator decomposition rate, which may lead to a 'dead end' polymerization scenario and limit the maximum monomer conversion that is theoretically achievable if the initiator depletes too quickly.[36, 37] Careful selection of the initiator concentration is also crucial because if it is too low, radical deficiency can lead to a low polymerization rate and/or limit monomer conversion. Conversely, too much initiator will eventually have a detrimental effect on the chain-end fidelity and dispersity of the synthesized polymer.[38] A screening study on initiator concentration and temperature was carried out and it was decided that $[M]_0$ / $[I]_0$ of 500 is the maximum allowable concentration before the control in polymerization deteriorates.[39] For our purpose, all the stock solutions were prepared at $[M]_0/[I]_0$ = 750 to ensure good control over the diblock copolymerization. For DMAEA, we experimented with higher initiator concentration ($[M]_0$ / $[I]_0$ = 300), due to literature reports of its lower polymerization rate.[40] To further enable maximum conversion, we leveraged understanding developed previously in our group which showed that a residence time equivalent to 4-5 times the half-life of the exogenous initiator being used is optimum.[18] This allows us to design a system that is applicable to all types of monomers being polymerized, as long as they are able to reach full conversion before initiator is used up. A range of acrylates and acrylamides are used to build up the material library as they have faster rates of propagation compared with other vinyl monomers. Further optimization of the system is required before it can be applied for slower propagating monomers like methacrylates and styrenics, therefore, they are excluded in this study. Due to a limited solubility of RAFT agent in the reaction solvent, the starting monomer concentration of stock solution 1 was kept at 4 M and to prevent reactor clogging, 2 M was chosen as the starting concentration for stock solution 2. On the other hand, $PEGMEA_{480}$ and DEGEEA stock solutions were prepared in lower concentration (1 M and 3 M respectively) due to their bulkiness. A summary of all reaction parameters trialled is given in **Table 1**.

View Article Online
DOI: 10.1039/D5SC07307C

Homopolymerization: Optimizing with timesweep kinetic screening

Based on the rationale outlined in the prior section, a timesweep kinetic screening experiment was carried out from a residence time (t_{res}) of 2 min, to capture the kinetic profile at lower conversion region, up to 40 min, which is roughly 5 times the half-life of AIBN at 100 °C. In most cases, it was observed that the monomer conversion largely plateaus after t_{res} of 25min (roughly 2 times the half-life of AIBN at 100 °C). Therefore, the timesweep screening was capped at 25 min, which also advantageously reduces experimental time. Details on the transient timesweep experiments can be found in literature.[9] The Python algorithm that controls this section of the setup consists of two parts: (1) a flow rate-varying program and (2) a data slicing and processing program. The flow rate-varying program controls the peristaltic pump to which stock solution 1 is connected (**Fig 4a**) and sets the flow rate according to residence time inputs by user. By referring to the timestamp of the raw IR data, data slicing is carried out automatically to select only the data during the transient periods (shaded regions on **Fig 4b**) of the experiment, and also (if needed), to isolate data during stabilization periods (circled regions on **Fig 4b**) for cross-validation purposes with NMR spectroscopic analysis. Subsequently, vinyl peak integration and monomer conversion calculation will be performed and a kinetic model with conversion *vs.* t_{res} data (**Fig 4c)** will be exported at the end of the experiment. The method to screen reactions only in the transient periods is established to deliver fast and reliable results, and indeed when data from the different transient sections is put together and recalculated for their respective reactor residence times, a smooth conversion vs time plot is obtained (**Fig. 3c**). EA, EGMEA, DEGEEA and $PEGMEA_{480}$ were chosen as the monomer for the first block due to their difference in hydrophilicity and molar mass and provide a useful

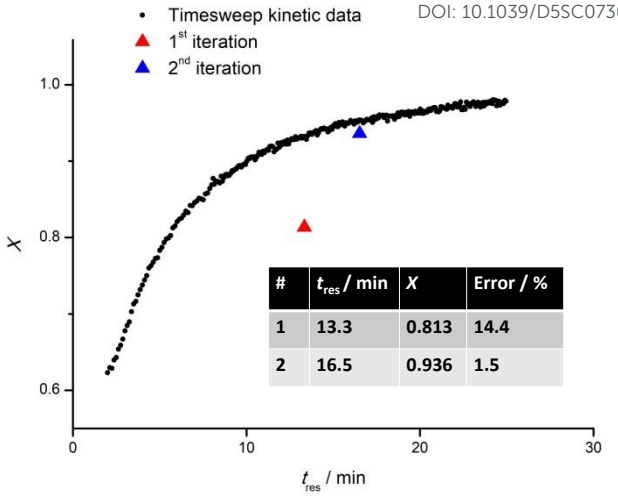

#	t_{res} / min	X	Error / %
1	13.3	0.813	14.4
2	16.5	0.936	1.5

Fig 3: Timesweep experiment of EA (DP_{Target} = 30) across a range of 2-25 min, followed by a fine-tuning experiment in which target *X* (95 %) was achieved in the second iteration, with a difference of less than or equal to 2 %.

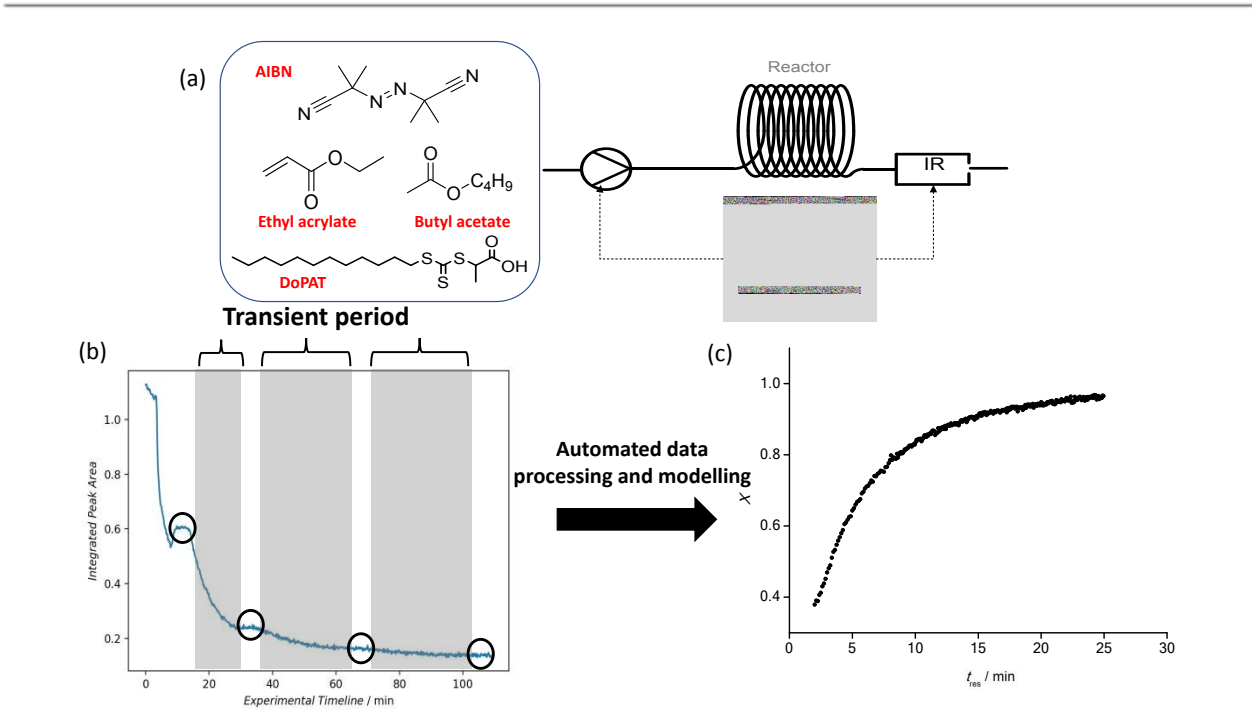

Fig 4: (a) Part of the automated setup for timesweep kinetic screening and self-optimising loop of homopolymerization. (b) Raw IR data collected and processed throughout a timesweep experiment of the polymerization of ethyl acrylate (EA). Circled region indicates stabilization period and sampling is carried out (optional), while shaded region indicates transient period. (c) Kinetic profile for the polymerization of EA, processed and exported from the Python program autonomously after the conclusion of timesweep experiment.

View Article Online
DOI: 10.1039/D5SC07307C

point from which a wide range of diblock copolymers can be subsequently prepared. To vary the chain length of the first block, the monomer/RAFT agent ratio was altered, while all the other process condition remains the same. The initiator to RAFT agent ratio was optimized to find a reasonable compromise between sufficiently high overall rate of polymerization and the fidelity of the obtained polymer (as expressed by the polymer dispersity). In the case of EA homopolymerization, the DP_{Target} was varied between 15 to 75. Both the observable rate of polymerization and maximum monomer conversion attainable (ranging from 89 % to 94 %) showed an increase with increasing DP_{Target}, which is consistent with prior observations.[13]

Next, the timesweep kinetic model obtained is used to predict the optimal residence time required for the reaction to reach a set monomer conversion, followed by iterative fine-tuning as needed (see below). This part of the process also serves as a corrective mechanism in the scenario where random errors (fluctuation in the ambient condition) or human errors (during preparation of the stock solution) are present, causing discrepancy from the previously obtained kinetic model. For this purpose, whenever the same monomer is being used as the first block, the user will be asked whether a timesweep experiment has been carried out before. If so, the data will be retrieved from a folder and used as a starting point from which the next experiment can be fine-tuned. To exemplify EA **(Fig 3)**, a new timesweep kinetic model for shorter t_{res} (2 – 25) min was obtained, and the maximum conversion achieved was around 97 %. When this kinetic data was retrieved for use in a new experiment, it was regressed linearly using the Scikit-learn package in Python, where -ln (1 - X) is set as the independent variable, and t_{res} as the dependent variable. t_{res} of 13.3 min was first predicted, which resulted in X = 81.3 %, a discrepancy of 14.4 % from the target X (95 %). The discrepancy could be due to various experimental factors like variation in the purity of chemicals used, difference in the ambient temperature or deviation of oil bath temperature from its setpoint. Moreover, the polymerization was assumed to follow first order kinetics, but in reality deviation from linearity was observed due to depletion of initiator at very high monomer conversion.[41] This shows that kinetics are only partially reproducible in a complex reactor setup due to outer influences. To tackle this, the self-optimising algorithm appended the latest data obtained to the previous dataset and assigned it with an increased sample weight of 200. This strategy introduced a significant positive bias to the latest data gathered. In this way, the resulting model was adjusted for the conditions in use. As exemplified in **Fig. 4,** a new t_{res} (16.5 min) was predicted by the updated model, resulting in X = 93.6 %, a discrepancy of only 1.5 % from the target, and less than the tolerable error margin (2 %) set by the user. Hence, the experiment was deemed successful. In all fine-tuning attempts, the targets were achieved in the first or second iteration, highlighting the high accuracy and also reproducibility of the timesweep approach. In the scenario where fine-tuning was carried out immediately after a timesweep experiment, the target conversion was achieved on the first iteration, as the reaction mixture was from the same source and the experimental errors outlined earlier were absent.

Diblock copolymerisation: Mixing efficiency and its influence on chain extension

With the ability to make homopolymers established, we next turned our attention to the preparation of BCPs. BCP synthesis can only work well if phases are mixed well. In a flow system, this usually can be problematic. Generally, chain extension requires a low viscosity solution (monomer) to mix with a comparatively high viscosity solution (homopolymer). Mixing two streams of such phases is not trivial because (i) typical continuous flow laboratory setups fall within the laminar flow regime and thus mixing is predominantly diffusion-controlled, irrespective of the type of mixer used[42] and (ii) the large molar mass of the macro-RAFT agent further impedes the mixing efficiency as its diffusion coefficient is exponentially smaller than other species in the reactor. We observed these limitations when trying to chain extend macro-RAFT agents of varying molecular weight, from DP_{Target} 25 to 75 derived from ethyl acrylate **(Figure S4)**. Shoulders were observable on the low molecular weight side of the elugrams of PEA_{50}-b-PBA_x and PEA_{75}-b-PBA_x, which overlapped with the macro-RAFT agents (PEA_{50} & PEA_{75}) used in both cases. This indicates incomplete chain-extension of significant amount of macro-RAFT agent in the reacting system. In diffusion terms, some of the macro-RAFT agent was not effectively mixed with monomer, and hence these chains could not grow further. Moreover, when introducing a micromixer, which usually introduces turbulent mixing, similar results were obtained **(Figure S5)**. However, PEA_{25}-b-$PEHA_x$ copolymers did not show this issue suggesting that improved homogeneity could be achieved with reduced molecular weight macro-RAFT agents. When swapping BA for MA, we found that co-polymers starting from a DP_{Target} PMA block of 50 chain-extended well, further validating the impact of the molecular weight contribution (MA having a lower molecular weight than EA).

Inspired by work from Chen and co-workers, and in an attempt to improve the chain extension of higher molecular weight macro-RAFT agents, we trialled the use of glass beads and an alumina packed bed column downstream of the Y-mixer as a means to improve turbulence.[43] Although some improvement in the molar mass distribution of the resulting diblock copolymers was observed, a significant pressure drop occurred as a result of the increased volume now introduced to the reactor. We next tried to introduce a greater mixing time via diffusion by adding extra volume between the mixer and reactor. [21, 34] This approach solved the homogeneity issue, indicated by absence of a low molar mass shoulder on the elugram of the synthesized diblock copolymers, but we saw a significant difference between the expected and obtained molar masses suggesting the mixing between macro-RAFT agent and stock solution were still sub-optimal. We therefore turned our attention to other types of mixers and found that the use of both a static micromixer (**Figure S5a**) and T-mixer (**Figure S5b**) led to a

View Article Online
DOI: 10.1039/D5SC07307G

surprising decrease in molar mass with increasing conversion for PEA_{50}-b-PMA_{50} BCPs. Since homogeneity didn't appear to be the cause (as indicated by absence of the MMD shoulders discussed above), it was hypothesized that the deviation was due to an incorrect molar ratio of macro-RAFT agent to monomer in the reactor. This can occur if the individual flow rates are too different, resulting in a significant pressure gradient that partially impedes the flow of one stream. Thus, a Y-piece mixer was chosen as it provides the least resistance to flow of the two streams. Further mixing was introduced by filling three channels of the auto-degasser with reagent prior to the timesweep experiment, under the same flow rates for both streams. This introduced sufficient reaction volume (3 × 12 ml) for the entire experiment, whilst ensuring consistency in the mixing ratio. When tested on the synthesis of PEA_{50}-b-PBA_{50} BCP, close agreement between the apparent numbered-average molar mass (M_n^{app}), determined from SEC, and theoretical number average molar mass (M_n^{theo}) was then satisfyingly observed (see **Figure S5c**).

Diblock copolymerization

Next, our experimental development progressed to stage 2 (chain extension), with the desired DP_{target} of the BCP inputted by the user. The macro-RAFT and monomer 2 stock solution streams are mixed prior to passing into reactor 2. The flow rate of the monomer in stock solution 2 is set again according to user specifications and a timesweep experiment is completed in the same way as for block one. Monomer conversion at specified t_{res} was determined by NMR spectroscopy and matched with the vinyl peak area as measured by FTIR spectroscopy. This allowed an empirical equation to be established and removed the need to establish individual IR calibration models for each monomer introduced to the polymer. Moreover, the combination of offline and online characterization tools provides a comprehensive kinetic profile of the reaction and more detailed characterization of the samples collected. Sample collection at different residence times (t_{res}) was facilitated by a liquid-handling autosampler. Since samples are taken in the stabilization period between set timesweep experiments, a series of samples with growing second blocks is obtained automatically, and hence different *DP* for the second block can be obtained without the need for multiple repeats of the same experiment.

By way of example, **Error! Reference source not found.** shows results from the preparation of a double hydrophobic BCP (PEA_{30}-b-PMA_{50}). **Error! Reference source not found.(a)** shows the plot of kinetic data (t_{res} *vs X*) obtained from the timesweep screening at t_{res} of 5 – 30 min. Conversions of up to 66 % were observed in this case, lower than those observed during the homopolymerization of each monomer. The lower polymerization rates observed are consistent with literature reports,[34] where the bulkiness (and hence slower diffusion rate) of the macro-RAFT agent impedes the overall rate of chain extension, thus requiring longer t_{res} to achieve monomer conversions comparable to a simple homopolymerization.[18] Moreover, the lower initiator ($[M]_0/[I]_0$ = 750) and monomer concentrations ($[M]_0$ = 1.33 M to 1.60 M) employed to both help maintain control of the diblock copolymerization whilst also prevent clogging of the reactor will also contribute to the slower reaction rate. Five samples were collected during the experiment, and the SEC traces of each are shown in **Error! Reference source not found.(b)**. The gradual shift of SEC traces without any observable shoulder indicates successful chain-extension of the macro-RAFT PEA_{50} and the increase in MMD was consistent with increasing monomer conversion. **Error! Reference source not found.(c)** shows good agreement between M_n^{theo} and M_n^{app} plots, and $Đ$ is less than 1.4 for all the BCPs, indicating good control of the polymerization.

Diblock copolymer material library construction

To demonstrate the versatility and robustness of the setup, we utilized it to synthesize 37 double hydrophobic, 40 amphiphilic and 18 double hydrophilic BCPs. Firstly, an EA block was chain extended with hydrophobic monomers (MA, BA or EHA) or

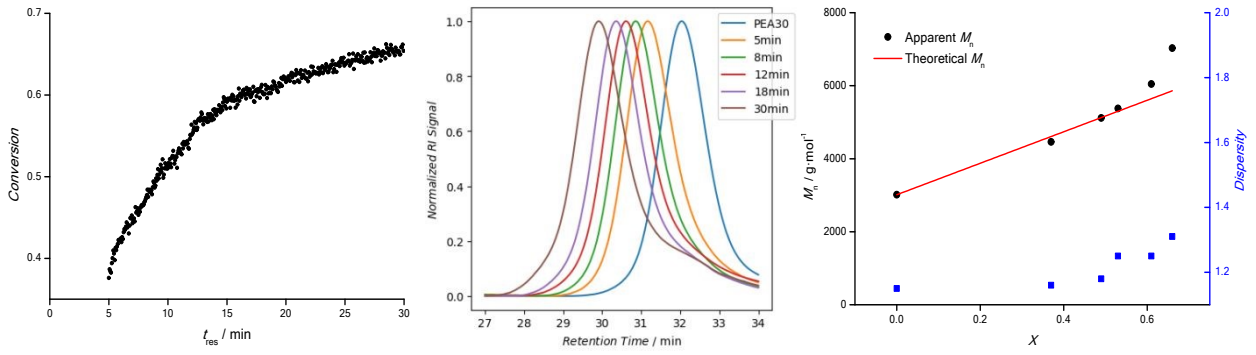

Fig 5: Data obtained from the synthesis of PEA_{30}-b-PMA_{50}): (a) Kinetic data from the timesweep experiment; (b) & (c) MMD and monomer conversion of PEA_{30}-b-PMA_{50} diblock copolymers, collected at different residence times, upon chain extension of PEA_{30} homopolymer. Conversion ranging from 30 to 70% was achieved.

View Article Online
DOI: 10.1039/D5SC07307G

hydrophilic monomers (DEGEEA, HEA, DMAC, DMAEA or $PEGMEA_{480}$) to form double hydrophobic or amphiphilic BCPs respectively. To make double hydrophilic BCPs, an EGMEA block was extended with AC, DMAC or HEA. For each starting homopolymer block, a series of BCPs was collected using a liquid-handling autosampler. This strategy, in tandem with the application of different types of monomers and by varying DP_{Target} of the first block, enables construction of a diverse BCP material library with minimal human intervention throughout the entire process flow **(Table 2)**. This library ranged in DP_{Target} of the first block from 15 – 75 and the second block from 30 – 100, with t_{res} between 2 - 50 min.

In this BCP library, monomer conversions ranged from 20 – 87 % and molecular weights from 1 800 g·mol^{-1} to 14 700 g·mol^{-1}, depending on the DP_{Target} in the first and second block, and the choice of t_{res} (and its X). For instance, the copolymer set with the smallest molar mass (1 800 – 4 900 g·mol^{-1}) was PEA_{15}-b-PBA_{30}, and the largest (8 700 – 14 700 g·mol^{-1}) was PEA_{50}-b-$PDMAC_{100}$. PEA_{15}-b-$P(PEGMEA_{480})_{30}$, showed a broader range of molar masses (5 000 – 10 400 g.mol^{-1}) due to the large molecular weight of $PEGMEA_{480}$ (M_n = 480 g·mol^{-1}), Narrow dispersity of all the BCPs synthesized ($Đ$ < 1.5, and in most cases < 1.3) indicates good control over the polymerization. It must be noted that exact molar mass determination of BCPs using SEC is inherently difficult without absolute molar mass detectors. This is further aggravated by the discrepancy in solvation and miscibility properties between the individual blocks, especially when mixed hydrophobic and hydrophilic BCPs are assessed.[44] As a result, the assumption of universal calibration in SEC does not hold true and the precise parameters required to use the Mark-Houwink-Sakurada (MHS) equation for each type of BCP are unavailable most of the time. Hence, a reasonable margin of error between the theoretical and apparent molar mass should be expected. Considering this, an average discrepancy of only 7.8 % between theoretical and apparent M_n is reasonable.

When comparing polymerisation kinetics for the monomers used, the hydrophilic monomers showed higher apparent polymerization rates, most notably with DMAC and HEA, where more than 80 % of monomer conversion was attained in 30 min. This could be attributed to the higher polarity of the monomers and hydrogen bonding between the monomer and polymer chain repeat unis.[45, 46] When comparing hydrophilic acrylates to acrylamides, by using PEA_{50}-b-$PDEGEEA_{50}$ and PEA_{50}-b-$PDMAC_{80}$ as the examples, the monomer conversion achieved in both experiments are 27 – 78 % and 22 – 87 % respectively. However, AC, despite being the same monomer class as DMAC, showed a lower rate and lower monomer conversion (X = 63 % at t_{res} = 30 min). This could be explained by a lower solubility of AC in the reaction solvent and may be resolved *via* use of a more polar solvent like DMSO.[47] In the synthesis of PEA_{75}-n-PBA_{75} BCPs, lower overall conversion (X = 49 % at t_{res} = 30 min) was observed. Rather than a systematic issue with the use of BA as a reactive monomer, this could be due to many experimental factors like fluctuations in the ambient temperature, inaccuracy in the temperature control of the hotplate being used or impurities present in the chemicals used. DMAEA was the only monomer with a significantly lower polymerization rate, with a maximum X of 32 % at 30 min when used to chain extend a PEA_{30} homopolymer, and similarly low conversion when used to extend a PEA_{50} homopolymer. This could be due to the reactivity of DMAEA (as a tertiary amine) towards the thiocarbonyl group of the RAFT agent[13] or its tendency to undergo self-catalysed hydrolysis of ester bonds in the side chains and would be worthy of future study.[48]

The samples collected during homopolymerization of $PEGMEA_{480}$ consistently showed a lower M_n^{app} than its M_n^{theo} **(Figure S6a)**. This is consistent with the literature, where branching in the polymer is reported to lead to a contraction in hydrodynamic volume and thus an underestimation of its apparent molar mass by SEC.[49, 50] When the same monomer was used for diblock copolymerization with a PEA_{15} homopolymer, M_n^{app} > M_n^{theo} at lower monomer conversion whilst the relationship inverts as more $PEGMEA_{480}$ is incorporated **(Figure S6b)**. The use of EHA also saw significant molecular weight discrepancies, potentially due to the hydrodynamic volume of the hydrophobic alkyl branching group when measured by SEC using a DMF eluent **(Figure S7b)**. Indeed, when re-analysed by SEC using a tetrahydrofuran (THF) eluent **(Figure S7a**, the M_n discrepancy reduced from 21 % to 6.6 %. Other individual copolymer samples that show a considerable M_n discrepancy (> 15 %) between their measured and apparent counterpart are PEA_{30}-b-PMA_{33} (t_{res} = 30 min) and PEA_{30}-b-$PDEGEEA_{50}$ (t_{res} = 30 min). This could be the cumulative effect of errors from sample preparation for analysis, inaccuracy in molar mass determination from the SEC and/or the standard error observed with NMR spectroscopic analysis. PEA_{44}-b-PMA_{38}, PEA_{50}-b-PBA_{50} and PEA_{50}-b-$PDEGEEA_{50}$ exhibited $Đ$ > 1.4. This was caused by targeting a larger DP_{Target} in both blocks. Thus, the $[CTA]_0$ / $[I]_0$ will inevitably decrease (as the $[M]_0/[I]_0$ is fixed to maintain the same overall polymerization rate), and control over the polymerization is reduced.[18] Furthermore, the bulkiness of monomer (DEGEEA), increased reaction mixture viscosity with higher DP_{Target} and monomer conversion in the second block, or random factors like fluctuation in ambient condition (heat and light exposure in the laboratory) can lead to impact of different extend on the control of the polymerizations. The latter factor is especially true as all the experiments were carried out at different times during the day or night, and each of them lasted more than 3 hours. Therefore, given the complexity and numerous factors affecting the control of polymerization, $Đ$ < 1.5 demonstrates satisfactory control across all polymerizations performed in this study. A reproducibility study was carried out for synthesis of PEA_{50}-b-PBA_{50}, conducted on three different days. The variance (in percentage) in the three sets of results was within the acceptable range (8% for the apparent rate constant), further exemplifying the potential of such system in accelerating material discovery. A detailed comparison of experimental runs for reproducibility elucidation is provided in Supporting Information (Figure S8 and Table S6).

View Article Online
DOI: 10.1039/D5SC07307C

ARTICLE

Table 2: Molecular weight distributions of all the diblock copolymers synthesized by the automated setup, at 100 °C. M_n^{theo} is calculated based on the conversion value from NMR spectroscopy. M_n^{app} and M_W^{app} are determined by SEC based on the Mark-Houwink parameters of PMMA. The average molar mass and monomer conversion for the first blocks are shown in the first row of each section, indicated by t_{res} = 0 min, while the subsequent rows show that for the diblock copolymers synthesized at different t_{res}. Double hydrophobic, amphiphilic and double hydrophilic diblock copolymers are indicated by blue, red and green lines respectively.

Diblock Copolymers	t_{res} /min	X	M_n /g	M_w /g	M_n^{theo} / g · mol^{-1}	$Đ$
PEA_{15}-b-PBA_{30}	0	0.89	1 800	2 000	1 700	1.10
	5	0.44	3 100	3 500	3 500	1.13
	8	0.58	3 800	4 200	4 200	1.12
	12	0.66	4 200	4 700	4 700	1.14
	18	0.67	4 500	5 200	5 200	1.15
	30	0.78	4 900	5 700	5 700	1.17
PEA_{15}-b-$PEHA_{30}$	0	0.89	1 800	2 000	1 700	1.10
	5	0.40	4 400	4 000	5 500	1.25
	8	0.56	5 100	4 900	6 300	1.25
	12	0.66	5 100	5 400	6 400	1.24
	18	0.69	5 300	5 600	6 400	1.21
	30	0.77	5 600	6 100	7 100	1.26
PEA_{30}-b-PMA_{50}	0	0.92	3 000	3 500	3 100	1.15
	5	0.37	4 500	5 200	4 600	1.16
	8	0.49	5 100	6 000	5 100	1.18
	12	0.53	5 400	6 700	5 300	1.25
	18	0.61	6 000	7 500	5 700	1.25
	30	0.66	7 000	9 200	5 900	1.31
PEA_{30}-b-PBA_{33}	0	0.92	3 000	3 500	3 100	1.15
	5	0.32	5 100	7 300	5 000	1.43
	8	0.46	5 900	8 100	6 000	1.42
	12	0.57	6 000	8 100	6 700	1.35
	18	0.65	6 200	8 100	7 200	1.31
	30	0.69	7 100	9 500	7 400	1.35
PEA_{44}-b-PMA_{38}	0	0.92	4 100	4 900	4 100	1.19
	5	0.51	5 300	7 000	5 700	1.33
	8	0.58	5 500	7 000	6 000	1.26
	12	0.62	6 500	8 400	6 100	1.30
	18	0.66	6 700	9 500	6 200	1.41
	30	0.73	7 000	9 700	6 500	1.39
PEA_{50}-b-PBA_{50}	0	0.94	5 500	6 200	5 100	1.11
	2	0.20	7 300	8 700	6 800	1.19
	5	0.39	8 200	9 800	8 000	1.19
	8	0.56	9 200	12 700	9 100	1.37
	12	0.70	10 200	15 000	10 000	1.47
	18	0.74	10 600	15 200	10 300	1.43
	30	0.79	11 000	16 500	10 600	1.50
PEA_{75}-b-PBA_{75}	0	0.93	7 800	8 700	7 300	1.12
	2	0.03	8 200	9 700	8 100	1.19
	5	0.09	9 000	10 900	8 700	1.21
	8	0.25	9 400	11 500	10 100	1.22
	12	0.35	9 700	12 600	11 100	1.30
	18	0.42	10 400	13 100	11 800	1.27
	30	0.49	11 000	13 700	12 500	1.22
PEA_{15}-b-$PDEGEEA_{30}$	0	0.89	1 800	2 000	1 700	1.10
	2	0.18	3 600	4 200	2 800	1.17
	5	0.49	5 200	6 100	4 600	1.17
	8	0.63	5 700	6 700	5 400	1.19
	12	0.71	5 900	7 100	5 800	1.21
	18	0.76	6 200	7 100	6 100	1.14

View Article Online
DOI: 10.1039/D5SC07307C

	30	0.77	6 300	7 400	6 200	1.17
PEA_{15}-b-$P(PEGMEA_{480})_{30}$	0	0.89	1 800	2 000	1 700	1.10
	2	0.11	5 000	6 000	3 500	1.20
	5	0.33	7 300	8 600	6 600	1.18
	8	0.50	8 800	10 400	9 000	1.18
	12	0.62	9 800	11 600	10 800	1.18
	18	0.69	10 100	12 200	11 800	1.21
	30	0.76	10 400	12 600	12 800	1.22
PEA_{30}-b-$PDEGEEA_{50}$	0	0.93	3 200	3 500	3 100	1.12
	2	0.11	5 700	6 600	4 200	1.16
	5	0.19	5 900	7 200	5 000	1.22
	8	0.40	7 400	9 200	7 000	1.24
	12	0.59	7 800	9 900	8 700	1.28
	18	0.69	8 300	10 500	9 700	1.27
	30	0.73	8 600	10 900	10 100	1.26
PEA_{30}-b-$PDMAEA_{30}$	0	0.93	3 200	3 500	3 100	1.12
	2	0.01	3 700	4 100	3 300	1.10
	5	0.06	3 900	4 300	3 600	1.12
	8	0.16	4 200	4 700	4 300	1.12
	12	0.17	4 400	4 900	4 400	1.11
	18	0.25	4 500	5 300	5 000	1.16
	30	0.32	4 700	5 400	5 500	1.15
PEA_{50}-b-$PDEGEEA_{50}$	0	0.94	5 700	6 400	5 100	1.07
	2	0.27	7 000	8 000	7 800	1.15
	5	0.48	10 500	13 500	9 800	1.28
	8	0.62	11 000	15 400	11 100	1.40
	12	0.69	11 100	16 400	11 800	1.48
	18	0.73	11 600	16 200	12 200	1.40
	30	0.78	12 400	18 000	12 600	1.46
PEA_{50}-b-$PDMAC_{100}$	0	0.91	5 300	6 000	5 100	1.13
	2	0.22	8 700	10 100	7 500	1.15
	5	0.52	11 600	13 100	10 400	1.14
	8	0.66	12 600	14 200	11 900	1.13
	12	0.77	13 500	15 500	12 900	1.15
	25	0.87	14 700	17 300	13 900	1.13
PEA_{50}-b-$PDMAEA_{80}$	0	0.91	5 300	6 000	5 100	1.13
	2	0.04	6 400	7 100	5 800	1.10
	5	0.12	7 100	8 000	6 700	1.12
	8	0.19	7 200	8 200	7 500	1.14
	12	0.24	7 300	8 700	8 100	1.19
	25	0.20	7 000	8 200	7 600	1.16
$PEGMEA_{30}$-b-$PDMAC_{50}$	0	0.94	3 700	3 800	4 000	1.15
	2	0.40	5 300	6 400	6 100	1.22
	5	0.60	6 300	7 800	7 100	1.18
	8	0.72	6 900	8 300	7 700	1.20
	12	0.73	6 900	8 200	7 700	1.18
	18	0.77	7 100	8 200	8 000	1.24
	30	0.82	7 300	8 500	8 200	1.23
$PEGMEA_{30}$-b-PAC_{50}	0	0.94	3 700	3 800	4 000	1.15
	2	0.23	5 000	5 600	5 000	1.13
	5	0.39	5 500	6 200	5 500	1.13
	8	0.45	5 600	6 400	5 800	1.15
	12	0.59	5 700	6 500	6 200	1.14
	18	0.62	5 700	6 700	6 300	1.17
	30	0.63	5 800	7 600	6 400	1.31
$PEGMEA_{30}$-b-$PHEA_{50}$	0	0.94	3 700	3 800	4 000	1.15
	2	0.19	5 500	6 600	5 200	1.20
	5	0.44	7 200	8 700	6 700	1.21
	8	0.50	7 600	9 000	7 000	1.18
	12	0.70	9 200	11 300	8 200	1.23
	18	0.73	9 100	10 900	8 400	1.19
	30	0.83	10 300	13 000	9 000	1.26

Conclusion

A fully automated setup for the high throughput synthesis of diblock copolymer libraries of varying polarities has been presented. This approach utilises in-line FTIR monitoring to optimize reaction kinetics in a data-centric manner, an in-line

View Article Online
DOI: 10.1039/D5SC07307G

degasser to remove manual deoxygenation processes and an autosampling method to minimise operator involvement throughput the entire process flow. A practical complication caused by the need for effective mixing of viscous macro-RAFT agent and less viscous monomer streams was overcome by mixing directly through the degasser. The versatility of this approach was then demonstrated by constructing a diblock copolymer material library comprising 7 sets of double hydrophobic, 7 sets of amphiphilic and 3 hydrophilic sets of diblock copolymers (95 samples). In addition, with the integration of in-line FITR, 17 sets of kinetic models were obtained for homopolymerization and diblock copolymerization respectively, providing comprehensive kinetic insights for all of the involved reactions.

This approach allows an "on demand" means to access a broad material library, removing some of the repetitive synthesis tasks typically observed with batch polymerizations. In principle the scope of this approach, though not tested in this report, could be expanded to collect products for extended times, allowing larger quantities of polymer (100 g or more) to be isolated.

Regardless, this automated reactor marks the full integration of self-driving lab principles and library synthesis for polymer discovery. In principle, after the user has specified their desired target polymer, the outlined reactor is able to run completely by itself, with human interaction only required for the loading of monomers and RAFT agent, and the characterization of the residual polymers. The entire process from optimization of the first block synthesis (achieving high conversion to facilitate good block copolymer formation) to block extension and systematic sampling is done by the synthesizer. The versatility of the system also means expansion with additional analytical instruments, pumps or reactors is possible, and it can be modified easily to serve different research purposes. For instance, via the addition of online SEC and pumps to control the monomer and RAFT agent flow rates individually, the system can be transformed into a self-driving lab for molecular weight targeting of the first and second block, by using the same optimization logic as the monomer conversion targeting that we have used in this study. A light source can also be integrated into the reactor setup for photopolymerization of slower propagating monomer, making polymerization of monomers such as methacrylates, styrene or others feasible.[51] As such, this system marks an important development step towards machines that can carry out complex polymer synthesis in a truly autonomous fashion.

Data availability

The data that support the findings of this study are available in the Monash research repository https://doi.org/10.26180/29396444.

Author contributions

Wei-Nian Wong: conceptualization, methodology, visualization, investigation, validation, and writing – original draft. **Daniel J. Phillips**: writing – reviewing and editing and supervision. Md **Taifur Rahman**: writing – reviewing and editing and supervision. **Tanja Junkers**: conceptualization, methodology, writing – reviewing and editing and supervision.

Conflicts of interest

The authors declare no conflict of interest.

Acknowledgements

This research was conducted by the Australian Research Council Industrial Transformation Training Centre Award (Green Chemistry in Manufacturing, project number IC190100034) and funded by the Australian Government.

Notes and references

1. A. El Jundi, S. J. Buwalda, Y. Bakkour, X. Garric and B. Nottelet, *Advances in Colloid and Interface Science*, 2020, **283**, 102213.
2. V. Agrahari and V. Agrahari, *Drug Discovery Today*, 2018, **23**, 1139–1151.
3. H.-C. Kim, S.-M. Park and W. D. Hinsberg, *Chemical Reviews*, 2010, **110**, 146–177.
4. S. M, J. S. Jayan and S. Appukuttan, *Journal of Molecular Liquids*, 2024, **412**, 125834.
5. L. Leibler, *Macromolecules*, 1980, **13**, 1602–1617.
6. D. J. Keddie, *Chemical Society Reviews*, 2014, **43**, 496–505.
7. A. C. Dimian, C. S. Bildea and A. A. Kiss, in *Computer Aided Chemical Engineering*, eds. A. C. Dimian, C. S. Bildea and A. A. Kiss, Elsevier, 2014, vol. 35, pp. 397–448.
8. M. B. Plutschack, B. Pieber, K. Gilmore and P. H. Seeberger, *Chemical Reviews*, 2017, **117**, 11796–11893.
9. J. Van Herck and T. Junkers, *Chemistry–Methods*, 2022, **2**, e202100090.
10. M. Rubens, J. Van Herck and T. Junkers, *ACS Macro Letters*, 2019, **8**, 1437–1441.
11. S. T. Knox, S. Parkinson, R. Stone and N. J. Warren, *Polymer Chemistry*, 2019, **10**, 4774–4778.
12. M. A. Bereś, B. Zhang, T. Junkers and S. Perrier, *Polymer Chemistry*, 2024, **15**, 3166–3175.
13. B. Zhang, A. Mathoor and T. Junkers, *Angewandte Chemie International Edition*, 2023, **62**, e202308838.
14. M. Rubens, J. H. Vrijsen, J. Laun and T. Junkers, *Angewandte Chemie International Edition*, 2019, **58**, 3183–3187.
15. J. J. Haven, J. Vandenbergh and T. Junkers, *Chemical Communications*, 2015, **51**, 4611–4614.
16. C. H. Hornung, X. Nguyen, S. Kyi, J. Chiefari and S. Saubern, *Australian Journal of Chemistry*, 2013, **66**, 192–198.
17. Z. Li, W. Chen, L. Zhang, Z. Cheng and X. Zhu, *Polymer Chemistry*, 2015, **6**, 5030–5035.
18. E. Baeten, J. J. Haven and T. Junkers, *Polymer Chemistry*, 2017, **8**, 3815–3824.
19. S. Parkinson, S. T. Knox, R. A. Bourne and N. J. Warren, *Polymer Chemistry*, 2020, **11**, 3465–3474.

20. J. Vandenbergh, T. de Moraes Ogawa and T. Junkers, *Journal of Polymer Science Part A: Polymer Chemistry*, 2013, **51**, 2366–2374.
21. P.-J. Voorter, G. Dev, A.-L. Buckinx, J. Dai, P. Subramanian, A. Kumar, N. R. Cameron and T. Junkers, *Chemical Science*, 2023, **14**, 8466–8473.
22. A. Kuroki, I. Martinez-Botella, C. H. Hornung, L. Martin, E. G. L. Williams, K. E. S. Locock, M. Hartlieb and S. Perrier, *Polymer Chemistry*, 2017, **8**, 3249–3254.
23. S. T. Knox, S. J. Parkinson, C. Y. P. Wilding, R. A. Bourne and N. J. Warren, *Polymer Chemistry*, 2022, **13**, 1576–1585.
24. M. Reis, F. Gusev, N. G. Taylor, S. H. Chung, M. D. Verber, Y. Z. Lee, O. Isayev and F. A. Leibfarth, *Journal of the American Chemical Society*, 2021, **143**, 17677–17689.
25. J. Van Herck, I. Abeysekera, A.-L. Buckinx, K. Cai, J. Hooker, K. Thakur, E. Van de Reydt, P.-J. Voorter, D. Wyers and T. Junkers, *Digital Discovery*, 2022, **1**, 519–526.
26. A. P. Grimm, S. T. Knox, C. Y. P. Wilding, H. A. Jones, B. Schmidt, O. Piskljonow, D. Voll, C. W. Schmitt, N. J. Warren and P. Théato, *Macromolecular Rapid Communications*, 2025, **n/a**, 2500264.
27. S. Lo, S. G. Baird, J. Schrier, B. Blaiszik, N. Carson, I. Foster, A. Aguilar-Granda, S. V. Kalinin, B. Maruyama, M. Politi, H. Tran, T. D. Sparks and A. Aspuru-Guzik, *Digital Discovery*, 2024, **3**, 842–868.
28. S. Mozharov, A. Nordon, D. Littlejohn, C. Wiles, P. Watts, P. Dallin and J. M. Girkin, *Journal of the American Chemical Society*, 2011, **133**, 3601–3608.
29. C. Sarosi, M. Moldovan, A. Soanca, A. Roman, T. Gherman, A. Trifoi, A. M. Chisnoiu, S. Cuc, M. Filip, G. F. Gheorghe and R. M. Chisnoiu, *Polymers*, 2021, **13**, 4415.
30. M. Brogly, S. Bistac and J. Schultz, *Polymer International*, 1997, **44**, 11–18.
31. I. M. Barszczewska-Rybarek, *Journal of Applied Polymer Science*, 2012, **123**, 1604–1611.
32. F. A. Rueggeberg, D. T. Hashinger and C. W. Fairhurst, *Dental Materials*, 1990, **6**, 241–249.
33. J. Zheng, Q. Liu, H. Zhang and D. Fang, *Spectrochimica Acta Part A: Molecular and Biomolecular Spectroscopy*, 2004, **60**, 3119–3123.
34. J. J. Haven, C. Guerrero-Sanchez, D. J. Keddie, G. Moad, S. H. Thang and U. S. Schubert, *Polymer Chemistry*, 2014, **5**, 5236–5246.
35. J. J. Haven, C. Guerrero-Sanchez, D. J. Keddie and G. Moad, *Macromolecular Rapid Communications*, 2014, **35**, 492–497.
36. T. Junkers and C. Barner-Kowollik, *Journal of Polymer Science Part A: Polymer Chemistry*, 2008, **46**, 7585–7605.
37. M. G. Joshi and F. Rodriguez, *Journal of Polymer Science Part A: Polymer Chemistry*, 1988, **26**, 819–826.
38. G. Gody, T. Maschmeyer, P. B. Zetterlund and S. Perrier, *Nature Communications*, 2013, **4**, 2505.
39. S. Perrier, *Macromolecules*, 2017, **50**, 7433–7447.
40. R. Sivkova, R. Konefal, L. Kostka, R. Laga, G. S. García-Briones, O. Kočková, O. Pop-Georgievski and D. Kubies, *Macromolecular Rapid Communications*, 2025, **46**, 2400640.
41. F. Ehlers, J. Barth, P. Vana, P. Vana, R. Storey, Y. Yagci, P. Nesvadba, B. Wayland, G. Moad, A. Goto and R. S. o. Chemistry, in *Fundamentals of Controlled/Living Radical Polymerization*, eds. N. V. Tsarevsky and B. S. Sumerlin, The Royal Society of Chemistry, 2013, DOI: 10.1039/9781849737425-00001, p. 0.
42. J. S. Vrentas and J. L. Duda, *Journal of Polymer Science: Polymer Physics Edition*, 1977, **15**, 417–439.
43. F. Zhong, F. Zhong, Y. Zhou and M. Chen, *Polymer chemistry.*, 2019, **10**, 4879–4886.
44. K. Philipps, T. Junkers and J. J. Michels, *Polymer Chemistry*, 2021, **12**, 2522–2531.
45. J. E. S. Schier, D. Cohen-Sacal and R. A. Hutchinson, *Polymer Chemistry*, 2017, **8**, 1943–1952.
46. A. Noguchi and M. Kuzuya, *Macromolecular Chemistry and Physics*, 2001, **202**, 1021–1030.
47. X. Liu, Q. Sun, Y. Zhang, Y. Feng and X. Su, *Molecules*, 2023, **28**.
48. R. Sivkova, R. Konefal, L. Kostka, R. Laga, G. S. García-Briones, O. Kočková, O. Pop-Georgievski and D. Kubies, *Macromolecular Rapid Communications*, **n/a**, 2400640.
49. T. Satoh and T. Kakuchi, *Macromolecular Bioscience*, 2007, **7**, 999–1009.
50. C. Gottschalk and H. Frey, *Macromolecules*, 2006, **39**, 1719–1723.
51. G. D. Ammini, J. P. Hooker, J. Van Herck, A. Kumar and T. Junkers, *Polymer Chemistry*, 2023, **14**, 2708–2716.

View Article Online
DOI: 10.1039/D5SC07307C

Data availability

The data that support the findings of this study are available in the Monash research repository https://doi.org/10.26180/29396444.